ORIGINAL ARTICLE

WILEY **MOLECULAR ECOLOGY**

Evolution of resistance to chytridiomycosis is associated with a robust early immune response

Laura F. Grogan[1,2,3] (iD) | Scott D. Cashins[1] | Lee F. Skerratt[1] | Lee Berger[1] | Michael S. McFadden[4] | Peter Harlow[4] | David A. Hunter[5] | Ben C. Scheele[1,6] | Jason Mulvenna[7,3]

[1]One Health Research Group, College of Public Health, Medical and Veterinary Sciences, James Cook University, Townsville, QLD, Australia

[2]Griffith Wildlife Disease Ecology Group, Environmental Futures Research Institute, School of Environment, Griffith University, Nathan, QLD, Australia

[3]Genetics and Computational Biology, QIMR Berghofer Medical Research Institute, Brisbane, QLD, Australia

[4]Taronga Conservation Society Australia, Mosman, NSW, Australia

[5]Ecosystems and Threatened Species, South West Region, Office of Environment and Heritage, NSW Department of Premier and Cabinet, Queanbeyan, NSW, Australia

[6]Fenner School of Environment and Society, Australian National University, Canberra, ACT, Australia

[7]School of Biomedical Sciences, The University of Queensland, Brisbane, QLD, Australia

Correspondence
Laura F. Grogan, Griffith Wildlife Disease Ecology Group, Environmental Futures Research Institute, School of Environment, Griffith University, Nathan, QLD, Australia.
Email: l.grogan@griffith.edu.au

Abstract

Potentiating the evolution of immunity is a promising strategy for addressing biodiversity diseases. Assisted selection for infection resistance may enable the recovery and persistence of amphibians threatened by chytridiomycosis, a devastating fungal skin disease threatening hundreds of species globally. However, knowledge of the mechanisms involved in the natural evolution of immunity to chytridiomycosis is limited. Understanding the mechanisms of such resistance may help speed-assisted selection. Using a transcriptomics approach, we examined gene expression responses of endangered alpine tree frogs (*Litoria verreauxii alpina*) to subclinical infection, comparing two long-exposed populations with a naïve population. We performed a blinded, randomized and controlled exposure experiment, collecting skin, liver and spleen tissues at 4, 8 and 14 days postexposure from 51 wild-caught captively reared infection-naïve adult frogs for transcriptome assembly and differential gene expression analyses. We analysed our results in conjunction with infection intensity data, and the results of a large clinical survival experiment run concurrently with individuals from the same clutches. Here, we show that frogs from an evolutionarily long-exposed and phenotypically more resistant population of the highly susceptible alpine tree frog demonstrate a more robust innate and adaptive immune response at the critical early subclinical stage of infection when compared with two more susceptible populations. These results are consistent with the occurrence of evolution of resistance against chytridiomycosis, help to explain underlying resistance mechanisms, and provide genes of potential interest and sequence data for future research. We recommend further investigation of cell-mediated immunity pathways, the role of interferons and mechanisms of lymphocyte suppression.

KEYWORDS
Batrachochytrium dendrobatidis, chytridiomycosis, gene expression, next-generation sequencing, resistance, transcriptomics

1 | INTRODUCTION

The emergence of biodiversity diseases that worsen the conservation status of wildlife species is of increasing global concern (Grogan

et al., 2014). Spread of chytridiomycosis, a skin disease caused by fungal pathogen *Batrachochytrium dendrobatidis* (Bd), has devastated amphibian species around the world (Skerratt et al., 2007), but is now endemic in most climatically suitable regions (Fisher, Garner, &

Walker, 2009; Kinney, Heemeyer, Pessier, & Lannoo, 2011; Murray et al., 2011). Despite endemism, many populations continue to be threatened by chytridiomycosis (Murray, Skerratt, Speare, & McCallum, 2009; Phillott et al., 2013; Scheele, Hunter, Skerratt, Brannelly, & Driscoll, 2015; Scheele et al., 2017; Skerratt et al., 2016). Development and implementation of *in situ* interventions for managing these populations are still in their infancy (Bosch et al., 2015; Scheele et al., 2014). Selection for evolved resistance or tolerance to disease has been suggested as a possible strategy for promoting long-term population persistence and assisting the successful repatriation of *ex situ* captive colonies (Scheele et al., 2014; Skerratt et al., 2016; Venesky, Mendelson, Sears, Stiling, & Rohr, 2012). The evolution of resistance or tolerance has been demonstrated in other wildlife (Atkinson, Saili, Utzurrum, & Jarvi, 2013), such as the resistance to bacterial infection with *Mycoplasma galliseptum* in the North American house finch (*Carpodacuc mexicanus*; Bonneaud et al., 2011).

Individual-, population-, and species-level differences in susceptibility to chytridiomycosis suggest immunologic management strategies are possible (Scheele et al., 2014; Searle et al., 2011). However, many nonimmune factors also determine disease manifestation (variations in autecology, behaviour, environment and pathogen strain; Berger, Marantelli, Skerratt, & Speare, 2005; Koprivnikar, Gibson, & Redfern, 2011; Murray & Skerratt, 2012; Rowley & Alford, 2007). The broad host and geographic range of chytridiomycosis has also made it difficult to draw parallels across species and systems and hence find generic solutions (Olson et al., 2013). The amphibian immune response to pathogens, similar to other vertebrates, is extremely complex, involving numerous cell types and hundreds of interacting molecular pathways (Murphy, 2012; Robert & Ohta, 2009). This complexity makes it difficult not only to isolate the effects of individual components, but also to understand their relative importance within the whole system (Ramsey, Reinert, Harper, Woodhams, & Rollins-Smith, 2010). Several immune determinants of susceptibility have been identified to date, including antimicrobial skin defence peptides, symbiotic skin bacteria and their antifungal metabolites, immune cells and their responses to Bd, stress metabolites and expression of major histocompatibility complex (MHC) genes (Bataille et al., 2015; Berger, Speare, & Skerratt, 2005; Cashins et al., 2013; Fites et al., 2013; Holden & Rollins-Smith, 2014; McMahon et al., 2014; Pask, Cary, & Rollins-Smith, 2013; Ramsey et al., 2010; Savage & Zamudio, 2011; Young et al., 2014).

Key elements of selecting for evolved resistance to chytridiomycosis involve (i) evidence for the evolution of resistance in amphibian populations, (ii) understanding the underlying mechanisms associated with evolved resistance and (iii) identification of molecular and genetic targets for marker-assisted selection (MAS)— an approach that has been successfully used for selecting disease resistance in plant and animal agriculture (Leeds et al., 2010; Ragimekula et al., 2013). Two studies have made initial progress towards these goals by examining MHC gene expression and correlating this with survival in clinical experiments and in wild populations (Bataille et al., 2015; Savage & Zamudio, 2011), indicating likely selection for resistance at the MHC locus. While such gene-targeted approaches can yield important information about the potential evolution of resistance (Meyer & Thomson, 2001), they may overlook the potentially multifactorial nature of protective immunity and other key components of the immune system that provide protection.

Dynamic gene expression in response to chytridiomycosis has been investigated with alternative nontargeted approaches in several studies (Ellison et al., 2014, 2015; Price et al., 2015; Ribas et al., 2009; Rosenblum, Poorten, Settles, & Murdoch, 2012; Rosenblum et al., 2009); however, none have examined the potential for evolution of resistance within species, nor related gene expression responses to demonstrated clinical survival. Early whole-genome microarray studies found little evidence for a robust immune response in skin, liver and spleen tissues of exposed frogs at various times since exposure (sampled at 3, 7, 16 and 42 days postexposure; DPE) in three susceptible species (*Xenopus (Silurana) tropicalis*, *Rana muscosa* and *R. sierrae*; Ribas et al., 2009; Rosenblum et al., 2009, 2012). In contrast, a recent transcriptomics study found high expression of immune-associated transcripts in the skin and spleen of moribund (sampled at 22–33 DPE) *Atelopus zeteki* (a highly susceptible species) in conjunction with decreased expression of lymphocyte-associated transcripts in the spleen (Ellison et al., 2014). Furthermore, when compared with two resistant (*Craugastor fitzingeri* and *A. callidryas*) and one other susceptible species (*A. glyphus*), Ellison et al. (2015) found comparatively lower levels of immune response in skin and spleen tissues of resistant species at peak infection loads (sampled at 33–62 DPE), although only susceptible species demonstrated suppression of splenic T-cell genes.

These apparently conflicting levels of immune response observed between the different studies may be associated with differences in sensitivity of the methodology (the former three used microarrays; Ribas et al., 2009; Rosenblum et al., 2012, 2009; while the latter two used highly sensitive RNA-seq; Ellison et al., 2014, 2015), differences in the inherent susceptibility of host species investigated (Searle et al., 2011), or the likely presence in the latter two studies of confounding immunopathology that may occur in late-stage infection (de Graaf et al., 2015). Host–pathogen infection interactions are highly temporally dynamic (Huang et al., 2011) and are often characterized by many nonprotective processes including escalating pathophysiology (disruption of homeostasis, tissue damage and bacterial co-infections) with increasing infection intensity, that may confound late-stage observations (Berger et al., 2005). Thus, while investigating putative immune mechanisms underlying clinically protective resistance, it is important to consider early subclinical responses. A recent RNA-seq study by Price et al. (2015) found a stronger (albeit small) transcriptional response at 4 DPE to Bd than to *Ranavirus* in liver tissue of *Rana temporaria* (a species relatively resistant to Bd but susceptible to *Ranavirus*); however, these results were not linked with clinical evidence for resistance and greater survival in individuals. These findings show that comparing the early transcriptomic response between frogs with differing clinical resistance to Bd has potential to identify novel and effective immunological changes that are not confounded by late-stage immunopathology.

In this study, we used a nontargeted transcriptomics approach to investigate underlying immune mechanisms that may be associated with the evolution of resistance to chytridiomycosis and may manifest in the early subclinical phase of infection. We examined infection responses in the alpine tree frog (*Litoria verreauxii alpina*) comparing frogs from a naïve population (Grey Mare) and from two populations that had been exposed to the fungus for approximately 20 years through many generations (Kiandra and Eucumbene). Unfortunately, at the time of our study there were no other known naïve populations available, so the lack of replication of the naïve population was beyond our control. We characterized differential gene expression between wild-caught captive-raised adult frogs comparing experimentally infected and uninfected frogs between populations, sampling three different immune-associated tissues (skin, spleen and liver) at various subclinical time points postexposure (4, 8 and 14 days). We examined infection intensities and compared our results with survival curves from a large experiment undertaken concurrently with frogs from identical clutches (Bataille et al., 2015; Grogan, 2014; Grogan et al., 2018). The novelty of our approach lies in analysing gene expression in frogs raised from naïve and long-exposed populations (approximately 8–10 generations) that were concurrently assessed for susceptibility by an infection experiment.

2 | MATERIALS AND METHODS

2.1 | Study subjects and husbandry

Fifty-one Bd-naïve adult alpine tree frogs (*L.v. alpina*) were raised in Bd-negative quarantine conditions from wild-caught egg masses until eight months postmetamorphosis (Scientific License number: S12848). The frogs were sourced from three geographically distinct populations around Kosciuszko National Park, New South Wales, Australia (Grogan et al., 2018). Two of the populations (Kiandra and Eucumbene) had been long-exposed to Bd and had experienced marked declines associated with the spread of Bd in the 1980s (Osborne, Hunter, & Hollis, 1999; Scheele et al., 2014), while a third population (Grey Mare) was naïve to the pathogen (Hunter et al., 2009; Scheele et al., 2016). The tissue-response experiment described here was performed concurrent with, under identical conditions, and using frogs from the same cohort as a larger exposure study examining survival responses. That survival experiment involved an additional 355 animals from three to four clutches from each of four populations (99 frogs from Eucumbene, 80 frogs from Grey Mare, 100 frogs from Kiandra and 76 frogs from an additional site Ogilvies).

Frogs were transferred to individual tubs several weeks prior to commencement of the exposure experiments to allow for acclimatization. Prior to and during the experiments, all frogs were housed individually under clean and controlled laboratory conditions, fed ad libitum, and observed daily by an experienced animal handler and/or veterinarian for health status and clinical signs of disease. Full methodological details for both tissue-response and survival experiments are presented by Grogan et al. (2018) (also see Bataille et al., 2015 and Grogan, 2014).

2.2 | Exposure experiment

Frogs were confirmed negative to Bd prior to the commencement of the experiments via qPCR (see below). The tissue-response experiment consisted of 18 frogs from each of Eucumbene and Kiandra populations (including six negative control animals from each population), and 15 frogs from Grey Mare (including three negative control animals; Table 1). These frogs were sourced from Kiandra clutch B, Eucumbene clutch D and Grey Mare clutch B (see Grogan et al., 2018). A Bd strain isolated nearby approximately 2 years before was used for inoculations (AbercrombieNP-*L.booroolongensis*-09-LB-P7), being maintained as described previously (Cashins et al., 2013). Thirty-six experimental animals in the tissue-response experiment and 278 frogs in the survival experiment were individually exposed to 750,000 zoospores in 25 ml dilute salt solution (DSS). Negative control group frogs were treated similarly, but were sham exposed with only DSS. Details of the survival experiment exposure are described by Grogan et al. (2018). Animal experiments were approved by James Cook University Animal Ethics Committee (A1589) and were performed in accordance with the welfare requirements of the funding grant provided by Morris Animal Foundation.

2.3 | Euthanasia, sampling and determining infection intensity via qPCR

A randomized block design was used to select 17 frogs (allocated among populations and treatment groups) for each of three sampling sessions (performed at 4, 8 and 14 DPE corresponding with subclinical infections). Immediately prior to euthanasia, frogs were swabbed to confirm infection status and quantify Bd infection intensity via

TABLE 1 Experimental design outlining the number of frogs from each population and treatment group (Bd-exposed or Bd-unexposed control) sampled at each time point postexposure

Populations	Exposure—Day 0 Total no. of exposed (total no. of control)[a]	Day 4 No. of exposed sampled (no. of control sampled)[b]	Day 8 No. of exposed sampled (no. of control sampled)[b]	Day 14 No. of exposed sampled (no. of control sampled)[b]
Grey Mare (clutch B)	12 (3)	4 (1)	4 (1)	4 (1)
Eucumbene (clutch D)	12 (6)	4 (2)	4 (2)	4 (2)
Kiandra (clutch B)	12 (6)	4 (2)	4 (2)	4 (2)
Total	36 (15)	12 (5)	12 (5)	12 (5)

[a]Total number of unexposed control frogs shown in parentheses.
[b]Number of unexposed control frogs sampled shown in parentheses.

qPCR, and mass and snout–urostyle length were recorded. Frogs were then humanely euthanized via double pithing, and a midline coeliotomy was performed for tissue collection. Tissues collected included ventral abdominal and thigh skin, liver and spleen, and these were immediately transferred to RNAlater (Qiagen) and refrigerated overnight at 4°C before being stored longer term at −80°C. Gender was ascertained via examination of coelomic reproductive organs and forelimb nuptial pads on males. In brief, for the concurrent survival experiment, frogs were observed daily and euthanized when they demonstrated clinical signs of disease (described in detail by Grogan et al., 2018). Bd infection intensity data (in zoospore equivalents, ZSE) were collected via swabbing with a sterile dry swab, which was then stored dry at 4°C before being analysed for Bd DNA with the TaqMan real-time qPCR protocol (following Garland, Baker, Phillott, & Skerratt, 2009; Hyatt et al., 2007). Individual swabs were analysed in triplicate, and each run included an internal positive control.

2.4 | RNA extractions and Illumina sequencing

Total RNA was isolated from skin, liver and spleen tissue samples following the manufacturer protocols for 5-Prime PerfectPure RNA Tissue kits for liver and skin samples and Qiagen RNeasy mini kits for spleen samples (the spleens were considerably smaller in volume), as described by Grogan et al. (2018). RNAstable plates (Biomatrica) were used to ship total RNA samples dry and at room temperature. Total RNA quality and quantity were determined via (i) Nanodrop 1000 (Thermo, DE, USA) spectrophotometer, (ii) fluorimetric Ribo-Green assay (Thermo, DE, USA) and (iii) capillary electrophoresis with Agilent BioAnalyzer 2100 (Agilent Technologies, CA, USA). Samples containing >1 μg total RNA and having an RNA integrity number (RIN) >8 passed quality control. Library preparation and sequencing were performed at the Minnesota BioMedical Genomics Centre, USA. Up to 12 samples were multiplexed on each flow cell lane, and sequencing was performed with the Illumina HiSeq 2000 (Illumina, San Diego, CA, USA) generating >10 million 100 bp paired-end reads for each sample. Base call data were demultiplexed with CASAVA software 1.8.2 (Illumina, San Diego, CA, USA), generating .fastq files for each sample (Grogan et al., 2018).

2.5 | Data preparation, transcriptome assembly and functional annotation

Sequence reads from each sample were examined for read quality using FastQC. TRIMMOMATIC 0.30 (Bolger, Lohse, & Usadel, 2014) was used to trim adapter sequences, crop random hexamers (Hansen, Brenner, & Dudoit, 2010), perform sliding window trimming (window size 4, required quality 15), trim flanking low-quality bases, and remove reads with length <75 bases, while retaining widowed reads. Digital normalization (DigiNorm; Brown, Howe, Zhang, Pyrkosz, & Brom, 2012) was used to remove read redundancy, and Bowtie (Langmead, Trapnell, Pop, & Salzberg, 2009) removed reads aligning to the Bd genome. We then generated de novo tissue-specific

transcriptome assemblies with Trinity (Haas et al., 2013; tissue-specific for logistical reasons). To reduce partial or erroneous contigs, we mapped reads back to the assembly and removed contigs with <4 reads per million mappable reads (Harrison, Mank, & Wedell, 2012; Moghadam, Harrison, Zachar, Székely, & Mank, 2013). Identification of the protein-coding regions in the assembled transcripts was performed using TransDecoder (Trinity). We then used BLAST2GO version 3.3 (Conesa et al., 2005), with basic linear alignment search tool (BLASTX) to assign sequences to an in-house anuran database consisting of the Amphibia subset of the National Center for Biotechnology Information (NCBI) nonredundant protein database. We functionally annotated each assembled transcript (gene) via BLAST2GO with data from the Gene Ontology [GO] consortium, Enzyme Code and Inter Pro (Jones et al., 2014) databases (detailed by Grogan et al., 2018). For the purposes of downstream interpretations, we considered BLASTX annotations with a minimum eValue of $\leq 1 \times 10^{-3}$ and mean sequence similarity ≥40%.

2.6 | Statistical analysis—differential gene expression, clustering and GO enrichment analyses

The R package RSEM (Li & Dewey, 2011) was used to quantify the abundance of genes and isoforms in individual frog tissue samples in combination with the above-described tissue-specific assembled transcriptomes, generating tables of transcript count data. The data for the three populations and three tissue types were analysed independently. EDGER from the Bioconductor suite (Robinson, McCarthy, & Smyth, 2010) was then used to identify statistically differentially expressed genes between experimental groups (independently for the various within-population comparisons), using raw gene read counts as recommended. Significantly dysregulated transcripts were identified as those with FDR < 0.05 using Benjamini–Hochberg multiple testing correction. We first compared the within-population pooled unexposed control frog samples with respective exposed frog samples taken at 4, 8 and 14 DPE within the three populations, to identify genes that were either up- or downregulated relative to the control baseline of homeostatic gene expression. We then performed GO term enrichment analysis (using Fisher's exact test and FDR < 0.05) on these sets of genes identified as differentially expressed from each time comparison to determine enriched functional profiles. We used the fully annotated tissue-specific transcriptomes as the reference sets for these analyses. As a quality control measure, we performed batch effect analysis on unexposed control frog samples from the three tissue types to identify any underlying systematic differences between sampling sessions (Note S1, Figure S1).

In a separate analysis, we performed Euclidean distance clustering to identify broad expression patterns of differentially expressed genes (categorized by population within tissue type), incorporating genes with FDR < 0.05 and $\log_2$ fold change ($\log_2$FC) > 1 (using Trinity and custom scripts). After manual selection of major clusters, we plotted heatmaps with individual frog samples (columns of the heatmaps) ordered by increasing infection intensity within sampling

period groups in time-series fashion ("heatmap.3" from R package GMD; Zhao & Sandelin, 2012). We similarly performed GO functional enrichment analysis on the resulting cluster groups (plus the full set of genes from all clusters), as above, against the respective tissue-specific transcriptome reference set.

To specifically examine the expression of immune-associated genes, we manually extracted and curated a list of differentially expressed genes with putative immune functions for each population and sampling session. For this list, we searched for an a priori defined list of terms related to expected immune functions from among annotations for each gene (derived from the BLASTX gene name/description and GO terms).

3 | RESULTS

3.1 | Experimental results

All 51 alpine tree frogs survived the duration of the tissue-response experiment (up to 14 DPE) without demonstrating clinical signs of chytridiomycosis (muscle weakness, lethargy, peripheral erythema or inability to maintain normal upright posture). Demographic data on the sampled frogs including infection intensities assessed via qPCR pre-euthanasia at time of sampling are listed in Table 2. Unexposed control group frogs remained uninfected for the duration of the experiment except for one indeterminate result (one well positive, <2 zoospore equivalents, ZSE [Lva010 from Kiandra sampled at 8 DPE]). Exposed frogs became infected (consistently testing positive except one indeterminate result [Lva399 from Kiandra sampled at 4 DPE] and one negative result [Lva076 from Grey Mare sampled at 8 DPE]), demonstrating variable but increasing Bd intensities through time. Mean capped intensities (when the results curve was truncated corresponding to the highest qPCR standard) were 34, 2,200 and 11,161 ZSE for 4, 8 and 14 DPE, respectively (without truncating for the highest qPCR standard the 14 DPE average increased to 21,482 ZSE). These infection intensities are comparable to those observed from wild alpine tree frogs (Scheele et al., 2015). Frogs from different populations did not differ significantly in their mean mass or snout–urostyle length (SUL; one-way ANOVA not assuming equal variances, $F = 0.938$, $p = .398$, 2 df for mean mass; $F = 2.423$, $p = .099$, 2 df for SUL). However, we detected a significant difference in log-transformed uncapped Bd infection intensities between exposed frogs from the three populations at 14 DPE with samples from long-exposed Kiandra demonstrating the lowest intensities ($F = 6.5924$, $p = .044$, 2 df for $\log_{10}[ZSE + 1]$; Table 2). In addition, an observable (but nonsignificant) trend indicated lower infection intensities throughout the three sampling sessions in frogs from the Kiandra population (Figure 1).

In the concurrent large survival experiment using other animals from these and additional clutches (Bataille et al., 2015; Grogan, 2014; Grogan et al., 2018), all frogs from the respective clutches died by 86 DPE except for one frog from Kiandra. However, mean survival time for frogs from Kiandra was greater than from populations Grey Mare and Eucumbene (Figure 2). Frogs from Kiandra

(Clutch B; $N = 20$; mean time to death for the 19 that died = 36 days) survived for significantly longer when compared with the other long-exposed population Eucumbene (Clutch D; $N = 19$; mean time to death = 28 days; $\chi^2 = 19$, $df = 1$, $p < .0001$; using the Mantel–Haenszel test; Harrington & Fleming, 1982), and the naïve population Grey Mare (Clutch B; $N = 20$; mean time to death = 27 days; $\chi^2 = 29.9$, $df = 1$, $p < .0001$). However, there was no evidence for a significant difference in time to death between frogs from Eucumbene and Grey Mare ($\chi^2 = 0.7$, $df = 1$, $p = .41$). Comprehensive raw data records for both these experiments are presented by Grogan et al. (2018) (also see Bataille et al., 2015 and Grogan, 2014).

3.2 | RNA-seq data, transcriptome assembly and annotation

Total RNA was successfully extracted from all 152 skin, liver and spleen tissue samples collected from frogs. The amount of total RNA extracted varied by tissue type and size; mean total RNA extracted was 81.27 μg for liver samples (SD 45.58 μg; $N = 51$), 19.76 μg for skin samples (SD 8.51 μg; $N = 51$) and 5.47 μg for spleen samples (SD 1.69 μg; $N = 50$). Of these samples, 148 passed quality control with a quantity >1 μg and RIN > 8. Shipping at room temperature using RNAstable plates did not adversely impact RNA quality or resuspended mass. All 16 Illumina HiSeq 2000 flow cell lanes generated > 160 million pass filter reads (>10 million reads per sample). Average number of raw reads per sample for liver was 15,819,807, SD 1,940,924, $N = 50$; for skin was 15,220,337, SD 4,778,641, $N = 51$; for spleen was 16,997,724, SD 2,302,778, $N = 50$; and overall total number of reads = 2,417,113,729. Phred quality scores were high within individual reads and across the data set (average Q-Score = 34.7; 99.9–99.99% base call accuracy). Trinity transcriptomes were assembled de novo for each tissue, yielding 21,269 Trinity "transcript clusters" (hereafter referred to as genes) for liver; 26,894 genes for skin; and 28,879 genes for spleen tissues (Table S1). These gene numbers are comparable with similar non-model amphibian species' de novo transcriptome assemblies (Ellison et al., 2015). Approximately two-thirds of assembled genes were annotated with at least one significant hit via BLASTX against the anuran nonredundant protein database (69.6% of total assembled genes from liver tissues, 66.7% skin, 64.9% spleen), and full gene ontology (GO) annotations were assigned to marginally fewer (57.3% of total assembled genes from liver tissues, 54.4% skin, 52.5% spleen).

3.3 | General differential gene expression trends

Comparison of gene expression levels between negative control (uninfected) and exposed frog groups revealed distinct grouping by population for all three tissue types using multidimensional scaling plots (Robinson et al., 2010; Figure 3). Comparing exposed with control samples on a time-series basis (samples from 4, 8 and 14 DPE versus controls within population and tissue type groups) revealed the highest numbers of differentially expressed genes at the late subclinical

TABLE 2 Demographic characteristics of study subjects (including sample size, treatment group, gender ratios, mean mass pre-euthanasia, mean snout–urostyle length pre-euthanasia and mean and median infection intensity pre-euthanasia)

| | Kiandra | | Eucumbene | | Grey Mare | | F value[a] | p value[a] | df[a] |
	Exposed	Control	Exposed	Control	Exposed	Control			
Sample size	12	6	12	6	12	3			
Gender[b]	2M, 4F, 6U	2M, 4U	4M, 5F, 3U	5F, 1M	4M, 6F, 2U	1M, 2F			
Mean mass pre-euthanasia	2.99	3.02	3.02	4.05	3.51	3.19	0.938	0.398	2
Mean SUL pre-euthanasia[c]	29.97	30.72	28.80	32.1	32.27	32.03	2.423	0.099	2
Mean ZSE pre-euthanasia[d]	2158.82	0.28	9442.36	0.00	12114.72	0.00	6.592[e]	0.044[e]	2[e]
Median ZSE pre-euthanasia	290.00	0.00	715.00	0.00	910.00	0.00			

[a]Statistics comparing means between populations (pooling exposed and control frog values) using one-way ANOVA, p value and df degrees of freedom.
[b]Gender represented by M for males, F for females and U for unknown gender.
[c]SUL is snout–urostyle length measured with Vernier callipers.
[d]ZSE is zoospore equivalents as measured by qPCR.
[e]Statistics refer to $\log_{10}$-transformed uncapped Bd infection intensities ($\log_{10}[ZSE + 1]$) between exposed frogs from the three populations at 14 DPE. Other sampling time comparisons were not significant.
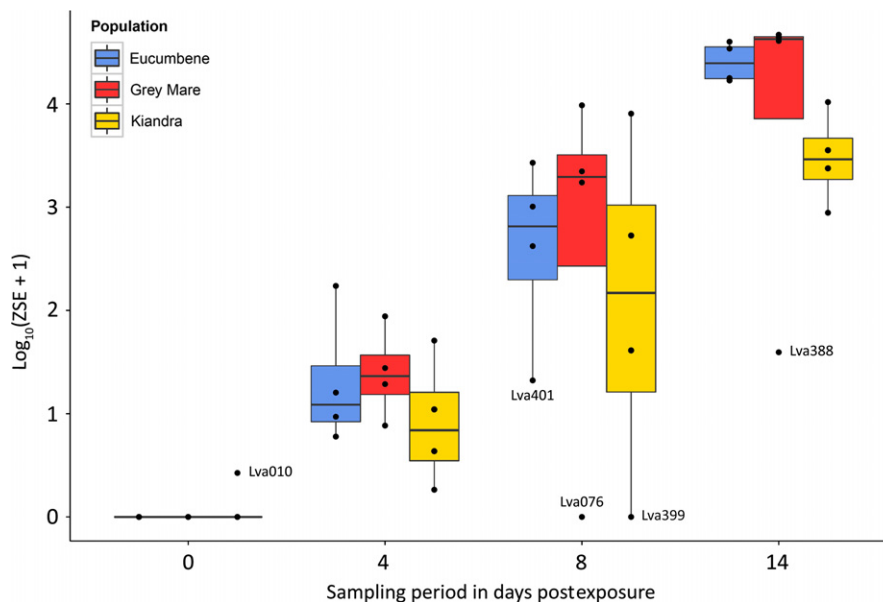
FIGURE 1 Box-and-whisker plots (with data points overlaid) of $\log_{10}$-transformed uncapped Bd infection intensities ($\log_{10}[ZSE + 1]$) for all 51 frogs at time of sampling (days postexposure; DPE), by population (using `geom_boxplot` from ggplot2 R package). Data from uninfected control frogs have been plotted as "zero" DPE (regardless of actual sampling date), for ease of comparison. Box hinges represent first and third quartiles, and middle represents the median. Whiskers extend 1.5 times the interquartile range of the hinge. Visually identified group outliers have been labelled with frog ID for ease of comparison (they were not removed from analyses)

infection time point (14 DPE) particularly in skin samples (Figure 4, Tables S2–S4). In addition, we observed a trend of decreasing gene dysregulation in the skin samples at 14 DPE in frogs from Grey Mare, Eucumbene and Kiandra, respectively. The range of gene expression fold-change [$\log_2 FC$] values varied between approximately 13 (upregulated relative to controls) and -13 (downregulated) for all differentially expressed genes from all tissue types (Tables S2–S4).

We found little overlap of differentially expressed genes between populations (with control samples taken as baseline) in both

the liver and spleen tissues, with greatest number of genes shared between the two long-exposed populations Eucumbene and Kiandra (Figures 5a,c; Micallef & Rodgers, 2014). However, many differentially expressed genes were found to be shared between populations in the skin samples, particularly between samples from the two most susceptible populations Grey Mare and Eucumbene (total of 1055 genes shared between Grey Mare and Eucumbene samples; Figure 5b). Venn diagrams for differentially expressed genes that were shared between populations separated by sampling time postexposure can be found in Figures S2–S4.
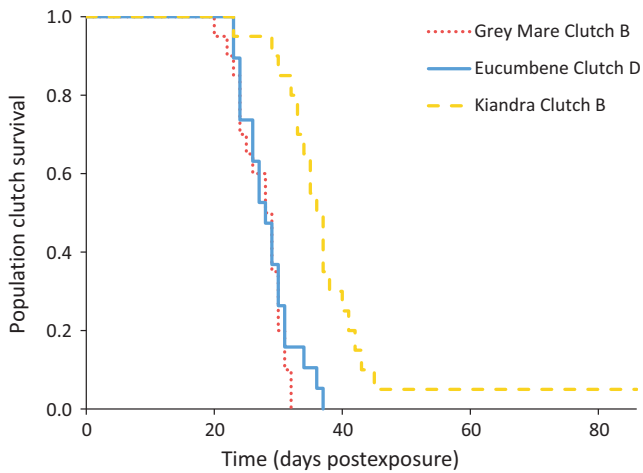
FIGURE 2 *L.v. alpina* population survival curves by population and clutch for the larger clinical experiment (Bataille et al., 2015; Grogan, 2014; Grogan et al., 2018). These animals were from the same respective clutches as the frogs used in the tissue-response experiment. The horizontal axis indicates survival in days postexposure (the experiment was terminated at 86 DPE for all groups)

3.4 | Clustering and gene ontology enrichment analysis

We identified 2–9 gene expression clusters for each tissue–population combination, and cluster expression patterns were most distinct in skin samples from Eucumbene and Grey Mare (Figure 6a,b). Heatmaps and cluster group fold-change averages (Figure 6, Table 3; Figure S5 and Table S5) revealed a gradually increasing time-series trend in gene expression in Eucumbene and Grey Mare clusters SkEuc1 and SkGre2, and a correspondingly decreasing trend in SkEuc2 and SkGre1 (Figure 6a,b; Table 3). A more distinct jump in

expression was observed for skin samples from Kiandra, whereby expression of genes in SkKia5 increased and SkKia4 decreased at 4 DPE relative to controls (SkKia1, SkKia2 and SkKia3 contained relatively few genes; Figure 6c and Table 3). This occurred despite one frog sampled in the 4 DPE group recording only a low and indeterminately positive infection intensity (Lva399).

GO enrichment analysis on major skin clusters increasing expression through time from the three populations (SkEuc1, SkGre2 and SkKia5) revealed significant over-representation of a relatively large group of immune-associated processes together with terms related to collagen metabolism, ion transport, molecule biosynthesis, and a variety of degenerative and salvage pathways (Figure 6; Figure S5 and Table S6). Significantly enriched immune-associated GO biological process terms in these clusters included, for example, "defence response," "inflammatory response," "immune response" (Figure S5 and Table S6). In contrast, immune-related processes were not represented in the main clusters with decreasing expression through time postexposure (SkEuc2, SkGre1, SkKia4). Other major groups of GO process terms were associated with epithelial homeostasis, water and ion transport and homeostasis, and musculoskeletal system processes. Significantly enriched GO biological process terms included, for example, "intercellular transport," "intracellular transport," "cellular water homeostasis" and "muscle contraction" (Table S6).

Although expression patterns were generally less clear in liver and spleen samples, significantly enriched immune-associated GO biological process terms were found in clusters that demonstrated a trend of increasing expression with time postexposure (LiEuc2, LiKia4, SpEuc2 and SpEuc5). However, unexpectedly, immune-associated terms were also significantly enriched in LiEuc1 (low expression at 14 DPE), LiGre1 (peak in expression at 8 DPE), LiKia1 (low expression at 4 DPE) and SpEuc3 (low expression at 14 DPE; Figure S5).
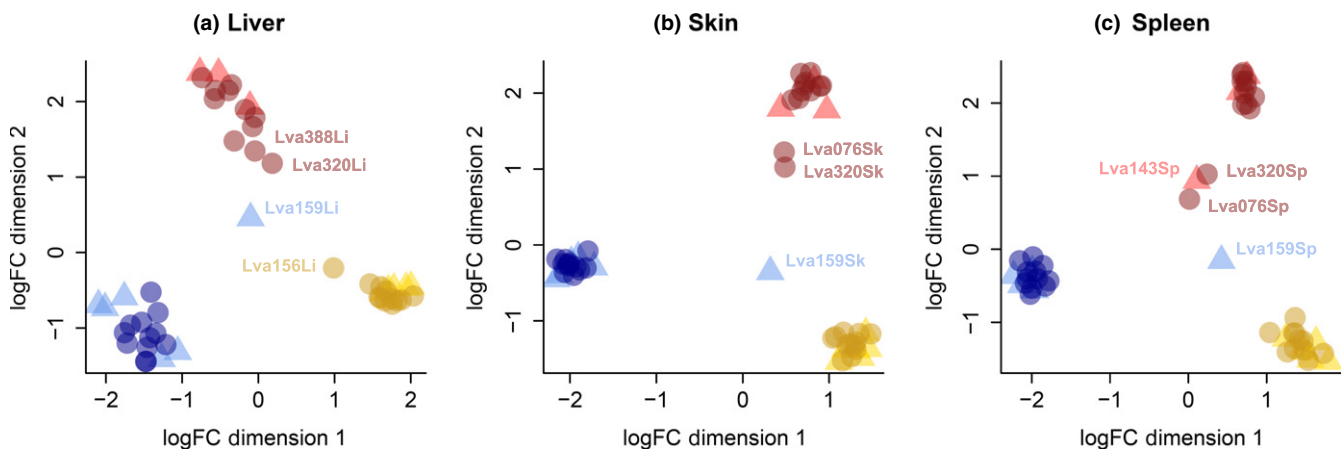

FIGURE 3 Unsupervised classical (metric) multidimensional scaling plots (using `plotMDS` and recommended settings from the Bioconductor package EdgeR) demonstrating leading log-fold changes between pairs of samples. Uninfected negative control frog samples (▲), Bd-exposed frog samples (●). Samples predominantly cluster by source population (colour groups: Eucumbene (blue), Grey Mare (red) and Kiandra (yellow)). (a) Liver samples, (b) skin samples and (c) spleen samples. Visually identified group outliers have been labelled with frog and tissue ID for ease of comparison (they were not removed from analyses)
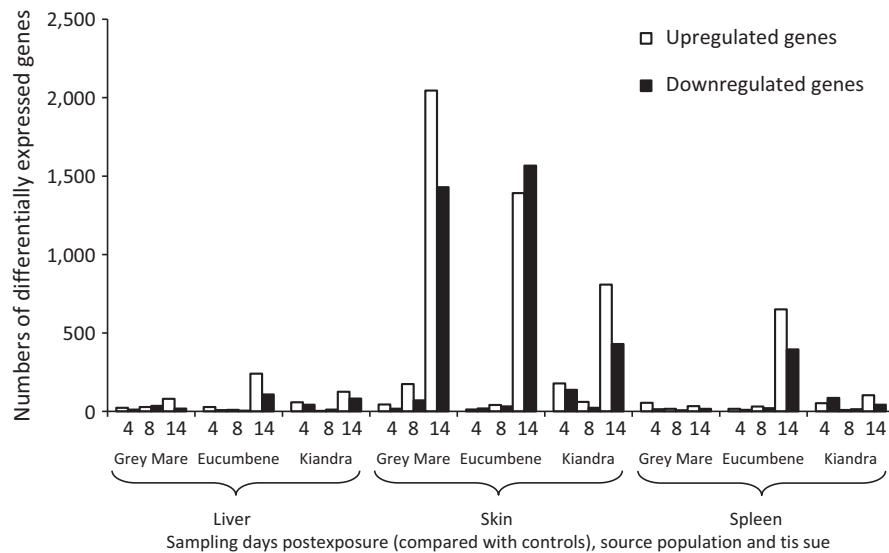
FIGURE 4 Numbers of up- and downregulated genes comparing uninfected negative control frog samples and Bd-exposed frog samples within-population at sampling periods postexposure, for all populations and tissues. Gene expression in skin samples from all three populations at 14 DPE were most highly dysregulated
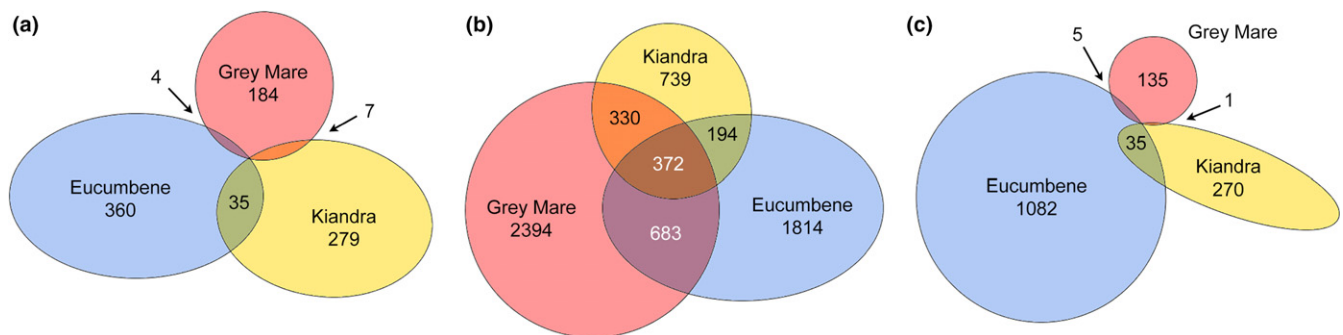

FIGURE 5 Venn diagrams comparing numbers of genes that were found to be dysregulated between populations within tissue groups (a) liver, (b) skin and (c) spleen (overlap indicates genes that were dysregulated in more than one population). Genes were classified as dysregulated if they were found to be significantly differentially expressed between uninfected negative control frog samples and Bd-exposed frog samples within-population among tissue samples

3.5 | Differential expression of immune-associated genes

Functional annotation of the differentially expressed gene lists (Tables S2–S4) revealed many genes with putative annotations related to the immune response (80 unique genes in liver, 629 in skin and 159 in spleen samples using our search term list; Figure 7 and Tables S7–S9). Gene functional homologies to all major recognized components of both the innate and adaptive vertebrate immune systems were identified. Genes associated with B and T lymphocytes including immunoglobulins (Igs), MHC, Fc receptors and NF-κB were dysregulated in exposed frogs. Genes associated with the classical, alternative and lectin complement pathways as well as lysozyme were found differentially expressed. We also identified many dysregulated genes related to antigen-presenting, phagocytic and cytotoxic cells including macrophages and neutrophils, as well as major groups of pattern-

recognition receptors including Toll-like and mannose receptors. There were also many examples of differentially expressed eicosanoid inflammatory mediators including leukotrienes, nitric oxide, as well as cytokines and chemokines including interferons (IFNs), interleukins (ILs) and tumour necrosis factors (TNFs). Log$_2$FC values for immune-associated genes varied from −8.6 to 7.8 for liver, from −10.1 to 9.0 for skin and −8.9 to 10.2 for spleen samples (Tables S7–S9).

Similarly to general gene expression trends, greatest numbers of immune-associated genes were expressed at the late subclinical infection time point (14 DPE) particularly in skin samples, with a similar trend observed of decreasing gene dysregulation in frogs from Grey Mare, Eucumbene and Kiandra, respectively (Figure 7). Many more immune-associated genes were found to be upregulated than downregulated when compared with unexposed control frogs (approximately three to four times; e.g., 671 upregulated compared with 200 downregulated immune-associated genes in the
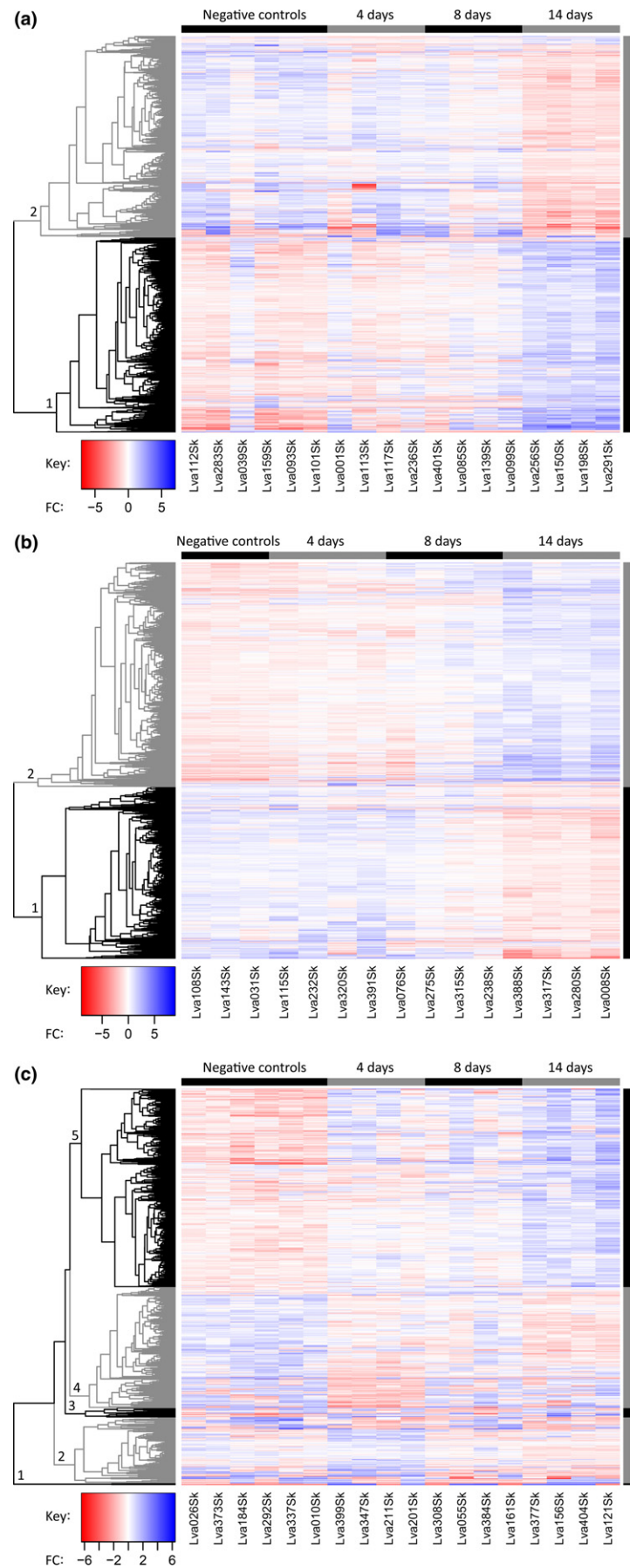
FIGURE 6 Heatmaps summarizing clusters (labelled at left) of differentially expressed genes (rows) clustered (via Euclidean distance algorithm) by expression pattern between samples within sample groups (days postexposure in columns) in the skin samples from frogs originating from (a) Eucumbene, (b) Grey Mare and (c) Kiandra. Control samples have been grouped together at the left, and samples within sample groups are arranged from left to right by increasing infection intensity at time of sampling (ZSE). Heatmaps for liver and spleen samples can be found in Figure S5

TABLE 3 Summary of mean expression patterns for the genes in each cluster at each time point, and corresponding example significantly enriched GO biological process terms for these clusters, among skin samples (see Table S6 for corresponding tables representing results from liver and spleen samples)

Cluster[a] ID	Mean centred log_2(fpkm + 1) by sample group[b]				No. of genes	No. GO terms (FDR < 0.05)	Example GO biological process terms[c]
	Control	4 days	8 days	14 days			
SkEuc1	−0.60	−0.19	−0.03	1.12	1,285	335	Collagen metabolic process; collagen catabolic process; multicellular organism metabolic process; multicellular organism catabolic process
SkEuc2	0.44	0.15	0.13	−0.95	1,325	176	Single-organism intercellular transport; intercellular transport; gap junction-mediated intercellular transport; glycerol transport
SkGre1	0.48	0.53	0.01	−0.90	1,430	196	Intracellular transport; single-organism intercellular transport; intercellular transport; gap junction-mediated intercellular transport
SkGre2	−0.73	−0.38	0.05	0.88	1,861	277	Collagen metabolic process; collagen catabolic process; multicellular organism metabolic process; multicellular organism catabolic process
SkKia1	−2.43	1.80	0.22	1.63	6	0	N/A
SkKia2	0.21	0.39	−0.20	−0.50	216	86	Cellular potassium ion homeostasis; sodium ion export from cell; establishment or maintenance of transmembrane electrochemical gradient; sodium ion export
SkKia3	−0.29	0.45	−0.64	0.63	31	0	N/A
SkKia4	0.52	−0.55	0.13	−0.35	394	9	Peptide cross-linking
SkKia5	−0.68	0.03	0.12	0.87	647	200	Collagen metabolic process; collagen catabolic process; multicellular organism metabolic process; multicellular organism catabolic process

[a]Clusters are defined by Euclidean distance clustering and manually selected using Trinity script `Manually_define_clusters.R` and labelled (see Figure 6 and Figure S5 for corresponding visual representations).

[b]Arithmetic mean of the centred log_2(fpkm + 1) expression values grouped by sampling time in days postexposure, from the output of Trinity script `Manually_define_clusters.R` ("Control" group includes all samples from unexposed frogs).

[c]Top four most significantly enriched GO Biological Process terms (where applicable; full list of overrepresented GO terms available in Table S5).

[d]N/A indicates that there were no GO Biological Process terms that were significantly enriched with FDR < 0.05 for the respective cluster.
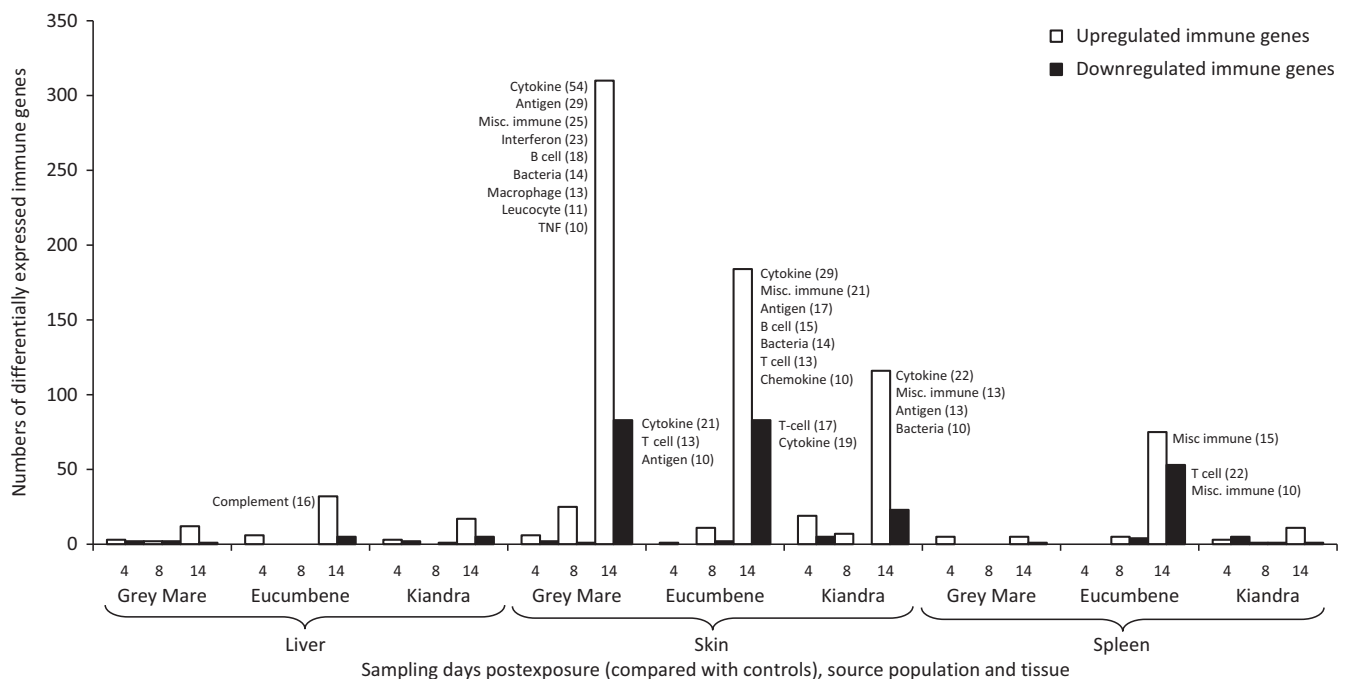

FIGURE 7 Numbers of up- and downregulated immune-associated genes comparing uninfected negative control frog samples and Bd-exposed frog samples within-population at sampling periods postexposure, for all populations and tissues. Major immune-associated gene groups have been labelled (using gene search terms; see Tables S2–S4 for more details), with numbers of differentially expressed genes in parentheses (where > 10 genes identified). Immune-associated genes were predominantly upregulated, particularly in skin samples from all three populations at 14 DPE

skin, Figure 7), and at least in the skin tissues, most of these downregulated genes were only distantly functionally related to immune processes (Tables S7–S9). Of particular note, however, a comparatively large number of T cell-associated genes were identified as downregulated in the skin of Grey Mare frog samples at 14 DPE, and the skin and spleen of Eucumbene frog samples at 14 DPE (Figure 7).

Of interest, the immune-associated genes with highest log_2FC values in the skin (highly upregulated compared with controls; $log_2FC > 4$) were found predominantly in the two more susceptible populations, Eucumbene and Grey Mare at 14 DPE (60 genes). The most highly upregulated of these included heat-shock proteins (log_2FC 9.0), IFN-induced genes (IFN-induced very large GTPase 1-like [log_2FC 8.8 and 7.8]) and antigen-presenting genes (log_2FC 8.7). Contrastingly, Kiandra frogs demonstrated marked upregulation only of MHC class II alpha chain genes in the skin at all time points post-exposure [log_2FC 6.3, 6.2 and 5.9].

3.6 | Differential expression of immune-associated genes in early subclinical infection associated with lower infection intensities and improved survival

Frogs from Kiandra demonstrated a broader representation of dysregulated immune-associated genes than frogs from the other two populations at 4 DPE (Note S2 for details). These included upregulated genes (predominantly in skin samples) associated with antigen-processing and presentation (MHC class II), cytokines (TNF, IL), the alternative complement pathway (factor B and a c3b analogue), the humoral immune response (Igs), and general inflammation and wound-healing processes. T-cell differentiation genes and IFN-associated GTPase genes were downregulated in all three tissues (e.g., IFN-induced very large GTPase [log_2FC -7.3] in the liver). Contrastingly, frogs from Grey Mare demonstrated marked upregulation of these IFN-induced GTPases in all three tissues at 4 DPE (ie, [log_2FC 8.8] in skin; interestingly, these genes were also upregulated at 8 and 14 DPE). Otherwise, frogs from Grey Mare and Eucumbene exhibited minimal early immune response to Bd infection compared with Kiandra. Some antigen-processing genes and cytokines were upregulated in the skin of Grey Mare frogs, while Eucumbene frogs had a strong early alternative complement pathway response in the liver.

Only a mild immune response was observed across tissues from Eucumbene and Kiandra frogs at the mid-subclinical infection time point (8 DPE), with upregulated genes including antigen-processing and presentation genes and cytokines from both populations, and alternative complement pathway and immunoglobulins from Kiandra frogs. Complement pathways were contrastingly downregulated in the skin and spleen of frogs from Eucumbene at 8 DPE. Frogs from Grey Mare demonstrated a comparatively more substantial immune response at 8 DPE, including upregulated genes associated with antigen-processing and presentation (MHC) and IFNs (total of 26 unique immune-associated genes identified in the skin samples).

4 | DISCUSSION

Frogs from a long-exposed population (Kiandra) of the alpine tree frog (*Litoria verreauxii alpina*) with a more disease-resistant phenotype displayed a more robust early (4 days postexposure; DPE) immune response at the level of gene expression in comparison with a susceptible Bd-naïve population (Grey Mare) and a susceptible long-exposed population (Eucumbene). Components of this early immune response may be vital for conferring chytridiomycosis resistance. Although the more susceptible populations exhibited larger immune responses at the late subclinical stage of infection (14 DPE), this finding is consistent with previous studies and suggests this late-stage response was nonprotective (Ellison et al., 2014, 2015).

In our experiment, we investigated infection intensities as well as functional immune response to subclinical chytridiomycosis (at 4, 8 and 14 DPE) at the site of infection (skin), and in two immune-related organs (spleen and liver). Frogs from Kiandra demonstrated a trend of lower infection intensities as early as 4 DPE onwards (significant at 14 DPE) when compared with frogs from the other two populations, suggesting their early manifestation of clinically protective resistance (Figure 1). Protective immune responses in amphibians are usually activated early in the infection process. For example, pathogen-induced antibodies to Frog Virus 3 were reported at 1 week postexposure and cell-mediated infection clearance occurred within 2–3 weeks (Gantress, Maniero, Cohen, & Robert, 2003; Robert et al., 2005). Frogs from Kiandra demonstrated a more robust immune response in early stage infection compared with the two more susceptible populations. Immune-associated genes that were upregulated relative to controls in the skin of frogs from Kiandra included representatives of both functioning innate and adaptive immune systems (antigen-processing and presentation genes, cytokines, alternative complement pathway genes, immunoglobulins, genes related to the humoral immune response and general inflammatory genes). However, there was some early evidence for the downregulation of T-cell differentiation genes and IFN-induced GTPase genes.

Overall, the baseline transcriptional response was divergent between the three populations, and although untested, this could be a result of long-term geographic isolation accompanied by a degree of parapatric speciation (Figures 3–5; Gavrilets, Li, & Vose, 2000). As expected from previous studies (Ellison et al., 2014, 2015; Rosenblum et al., 2009), our gene expression results from the late subclinical infection stage (14 DPE) were the most highly dysregulated, particularly so in skin samples. However, the trend in the numbers of dysregulated genes at 14 DPE was negatively associated with survival and infection intensity results among populations. Skin samples from Grey Mare, the Bd-naïve and most susceptible population, demonstrated the highest number of differentially expressed genes at the late subclinical time point with the greatest number of dysregulated immune-associated genes (Figure 7). In contrast, skin samples from Kiandra, the most resistant and one of the long-exposed populations, demonstrated the lowest level of differentially expressed genes (including immune-associated genes) at 14 DPE. These findings are consistent with the results from Ellison et al. (2015) where

more susceptible species were found to have a more dysregulated immune response than resistant species at a later stage of infection. Indeed, Ellison et al. (2014) found a marked transcriptional response of immune-associated genes in moribund frogs even in the highly susceptible species, *Atelopus zeteki*. We speculate that the observed highly dysregulated gene expression at 14 DPE, particularly in highly infected Grey Mare and Eucumbene populations, may either represent immunopathology (a dysregulated and damaging immune response), or a protective response to marked epithelial disruption. Epidermal damage occurs as Bd burdens increase and includes erosions, microvesicles, and less frequently ulcerations and bacterial infections that may be associated with cellular inflammation (Berger et al., 2005; Brutyn et al., 2012).

Dysregulated genes with functional homology to all major components of the vertebrate immune system were identified by gene ontological annotation of our tissue transcriptomes. The majority of these genes were upregulated in skin samples from the late subclinical stage of infection in the most susceptible populations Grey Mare and Eucumbene (Figure 7). A correspondingly broad range of immune-associated GO biological process terms was identified from skin samples in association with distinct gene clusters that exhibited increased expression with time postexposure. Notably, where heatmaps revealed a gradual increase in gene expression in these clusters from Grey Mare (SkGre2) and Eucumbene (SkEuc1), the corresponding cluster from Kiandra (SkKia5) increased more noticeably from 4 DPE, indicating an earlier immune response to Bd consistent with our trend of lower infection intensities and improved survival times (Figure 6, Table 3; Figure S5 and Table S6).

Skin clusters that exhibited decreased expression with time postexposure from all three populations were significantly enriched for predominantly homeostatic mechanisms, water and ion transport, musculoskeletal system processes and cardiovascular system processes related to conduction, contraction and regulation of heart rate (Figure S5 and Table S6). These findings likely constitute essential mechanisms underlying the observed late-stage clinical signs of chytridiomycosis which include skin ulceration and sloughing, ion loss, dehydration, lethargy and bradycardia, ultimately leading to asystolic cardiac arrest and mortality (Voyles et al., 2009, 2012). Cluster expression patterns from liver and spleen tissues were much less distinct in all three populations, with more clusters identified, and fewer significantly enriched GO terms. While some liver and spleen clusters with increasing expression through time also demonstrated significant enrichment for immune-associated GO terms, several other clusters with immune terms exhibited peaks or dips in expression at various time points postexposure, indicating that immune gene expression is comprised of a complex and dynamic network of immune signals varying between tissues over time.

Interestingly, we observed the downregulation of many lymphocyte-associated (particularly T cell related) genes in the skin samples of infected Grey Mare frogs at 14 DPE, and the skin and spleen of infected Eucumbene frogs at 14 DPE (Figure 7). One spleen sample cluster (SpEuc3) that exhibited decreased expression over time was significantly enriched for numerous T cell-associated processes

(Figure S5g). There was also some evidence for T-cell suppression in frogs from Kiandra. These findings are consistent with the results of Ellison et al. (2014), and previous findings of in vitro lymphocyte suppression mediated by a putative Bd-secreted virulence factor (Fites et al., 2013). T cell-associated cell-mediated immunity is likely to be especially important for intracellular pathogens such as Bd (Rollins-Smith et al., 2009), and involves differentiation of T lymphocytes into cytotoxic T cells which recognize and stimulate apoptosis of infected host cells, or phagocytosis by cells of the innate immune system. Downregulation of T cell-associated genes likely cripples the longer term amphibian adaptive immune response to chytridiomycosis, despite an otherwise highly upregulated immune system. Our result is also consistent with (i) the lack of cellular inflammation around sites of Bd infection (Berger et al., 2005) and (ii) reinfection experiments where highly effective adaptive immunity was not demonstrated in the species tested (Cashins et al., 2013; McMahon et al., 2014). We speculate that although frogs from the Kiandra population demonstrated a robust early immune response to Bd, the efficacy of cell-mediated immunity may have been stifled by Bd-associated suppression of the adaptive immune system, preventing resolution of infection in the longer term (in the survival study all but one of the frogs from Kiandra Clutch B died by 86 days postexposure although they survived on average longer than frogs from the other two populations; Bataille et al., 2015; Grogan, 2014).

Of particular interest, downstream processes of IFN were downregulated in all three tissues of frogs from Kiandra at 4 DPE. This finding is in direct contrast to the marked upregulation of IFN-induced genes in all three tissues of Grey Mare frogs throughout infection [several genes with $log_2FC > 5$], and the study by Price et al. (2015) where 11 of 29 annotated upregulated transcripts in liver samples from the Bd vs control comparison at 4 DPE represented similar IFN-induced genes. Frogs from Eucumbene demonstrated no such clear signal. IFN-γ is of central importance for nonspecific macrophage-associated cell-mediated immunity, although it may also be involved with antibody-associated cytotoxicity and has been linked with some autoimmune processes (Farrar & Schreiber, 1993). Interferon-induced GTPases play an important role in autonomous somatic cell immunity and may promote autophagy of intracellular microbial pathogens (Kim, Shenoy, Kumar, Bradfield, & MacMicking, 2012). The marked early upregulation of IFN-induced pathways (this study and Price et al., 2015) in conjunction with lymphocyte suppression and clinical evidence of susceptibility in frogs from Grey Mare suggests that (i) these responses are misdirected and insufficiently protective against Bd, and (ii) these pathways may play a more fundamental role in pathogenesis. Otherwise, frogs from Grey Mare exhibited only mild evidence of an early immune response to Bd infection compared with those from Kiandra, while frogs from Eucumbene demonstrated an early classical complement response in the liver (Note S2 and Tables S7–S9).

In the concurrent clinical survival study (Bataille et al., 2015; Grogan, 2014; Grogan et al., 2018), frogs from long-exposed Kiandra (including those from Clutch B) survived significantly longer than frogs from the two other populations (Figure 2), which may be

consistent with the evolution of resistance in frogs from Kiandra over approximately 20 years of intergenerational exposure to Bd. Interestingly, the Eucumbene population was also long-exposed; however, frogs from Eucumbene were found to be comparatively susceptible to Bd. We acknowledge the caveat of working with a small number of populations, which was necessary for logistic feasibility. We also acknowledge the lack of replication of our naïve population, a limitation that was beyond our control, but that potentially confounds infection history with unidentified causes of population variation in immunity. However, these caveats do not negate the value of our study because our findings relate the degree of observed clinical resistance to the underlying transcriptomic responses of the respective populations, rather than relying on long-term infection history as the explanatory factor.

An accompanying field study (Scheele et al., 2015) suggests that a likely mechanism for continued persistence of these populations despite high Bd-associated adult mortality is high compensating recruitment. Scheele et al. (2015) found a predominance of 2-year-old adults in the long-exposed populations, indicating that the majority of adults die during their first breeding season. Behavioural and life history characteristics of juvenile *L. v. alpina* mean that frogs do not commonly become infected prior to returning to the pond to breed. If adults typically breed successfully prior to succumbing to chytridiomycosis, this may reduce the selection pressure acting on disease resistance traits, resulting in poor evolution of immunity in this species.

This is the first study to identify underlying immune mechanisms at the early subclinical stage of infection that may be related to evolved resistance to Bd. Multiple lines of evidence demonstrated that a more resistant amphibian phenotype from an evolutionarily long-exposed population had an early immune response at the level of gene expression, which likely explains the reduced early Bd infection intensities and extended survival. Additionally, our results were consistent with Bd-associated lymphocyte suppression and raise questions about the role of IFN-induced pathways in Bd pathogenesis. We recommend future studies target pathways involved in cell-mediated immunity to elucidate the mechanisms underlying early responses to infection, the role of cytokines, such as IFN-γ and host-mediated T-cell suppression.

CONFLICTING INTERESTS

The authors declare no conflicting interests.

AUTHOR CONTRIBUTIONS

L.F.G., S.D.C, L.F.S. and L.B. designed research; D.A.H. and B.C.S. provided field knowledge and experience; L.F.G., S.D.C. and D.A.H. collected the amphibians; M.S.McF. and P.H. provided animal husbandry assistance and advice; L.F.G and S.D.C. performed the clinical experiment and collected samples; L.F.G. performed the RNA extractions; L.F.G. and J.M. performed the bioinformatics analyses; all authors discussed interpretation of results; L.F.G. wrote the manuscript draft; and all authors revised the manuscript drafts.

ORCID

Laura F. Grogan http://orcid.org/0000-0002-2553-7598

REFERENCES

Atkinson, C. T., Saili, K. S., Utzurrum, R. B., & Jarvi, S. I. (2013). Experimental evidence for evolved tolerance to Avian Malaria in a wild population of low elevation Hawai'i 'Amakihi (*Hemignathus virens*). *EcoHealth*, 10, 366–375. https://doi.org/10.1007/s10393-013-0899-2

Bataille, A., Cashins, S. D., Grogan, L., Skerratt, L. F., Hunter, D., McFadden, M., . . . Bell, S. (2015). Susceptibility of amphibians to chytridiomycosis is associated with MHC class II conformation. *Proceedings of the Royal Society B-Biological Sciences*, 282, 9.

Berger, L., Marantelli, G., Skerratt, L. L., & Speare, R. (2005). Virulence of the amphibian chytrid fungus *Batrachochytrium dendrobatidis* varies with the strain. *Diseases of Aquatic Organisms*, 68, 47–50. https://doi.org/10.3354/dao068047

Berger, L., Speare, R., & Skerratt, L. F. (2005). Distribution of *Batrachochytrium dendrobatidis* and pathology in the skin of green tree frogs *Litoria caerulea* with severe chytridiomycosis. *Diseases of Aquatic Organisms*, 68, 65–70. https://doi.org/10.3354/dao068065

Bolger, A. M., Lohse, M., & Usadel, B. (2014). TRIMMOMATIC: A flexible trimmer for Illumina sequence data. *Bioinformatics*, 30, 2114–2120. https://doi.org/10.1093/bioinformatics/btu170

Bonneaud, C., Balenger, S. L., Russell, A. F., Zhang, J., Hill, G. E., & Edwards, S. V. (2011). Rapid evolution of disease resistance is accompanied by functional changes in gene expression in a wild bird. *Proceedings of the National Academy of Sciences of the United States of America*, 108, 7866–7871. https://doi.org/10.1073/pnas.1018580108

Bosch, J., Sanchez-Tomé, E., Fernández-Loras, A., Oliver, J. A., Fisher, M. C., & Garner, T. W. (2015). Successful elimination of a lethal wildlife infectious disease in nature. *Biology Letters*, 11, 20150874. https://doi.org/10.1098/rsbl.2015.0874

Brown, C. T., Howe, A., Zhang, Q., Pyrkosz, A. B., & Brom, T. H. (2012). A reference-free algorithm for computational normalization of shotgun sequencing data. *arXiv e-print*. 1203.4802v1202 [q-bio.GN].

Brutyn, M., D'Herde, K., Dhaenens, M., Van Rooij, P., Verbrugghe, E., Hyatt, A. D., & Martel, A. (2012). *Batrachochytrium dendrobatidis* zoospore secretions rapidly disturb intercellular junctions in frog skin. *Fungal Genetics and Biology*, 49, 830–837. https://doi.org/10.1016/j.fgb.2012.07.002

Cashins, S. D., Grogan, L. F., McFadden, M., Hunter, D., Harlow, P. S., Berger, L., & Skerratt, L. F. (2013). Prior infection does not improve survival against the amphibian disease chytridiomycosis. *PLoS One*, 8, 7.

Conesa, A., Götz, S., García-Gómez, J. M., Terol, J., Talón, M., & Robles, M. (2005). BLAST2GO: A universal tool for annotation, visualization and analysis in functional genomics research. *Bioinformatics*, 21, 3674–3676. https://doi.org/10.1093/bioinformatics/bti610

de Graaf, H., Pai, S., Burns, D. A., Karas, J. A., Enoch, D. A., & Faust, S. N. (2015). Co-infection as a confounder for the role of *Clostridium difficile* infection in children with diarrhoea: A summary of the literature. *European Journal of Clinical Microbiology & Infectious Diseases*, 34, 1281–1287. https://doi.org/10.1007/s10096-015-2367-0

Ellison, A. R., Savage, A. E., DiRenzo, G. V., Langhammer, P., Lips, K. R., & Zamudio, K. R. (2014). Fighting a losing battle: Vigorous immune response countered by pathogen suppression of host defenses in the chytridiomycosis-susceptible frog *Atelopus zeteki*. *G3-Genes Genomes Genetics*, 4, 1275–1289.

Ellison, A. R., Tunstall, T., DiRenzo, G. V., Hughey, M. C., Rebollar, E. A., Belden, L. K., & Zamudio, K. R. (2015). More than skin deep: Functional genomic basis for resistance to amphibian chytridiomycosis. *Genome Biology and Evolution*, 7, 286–298. https://doi.org/10.1093/gbe/evu285

Farrar, M. A., & Schreiber, R. D. (1993). The molecular cell biology of interferon-gamma and its receptor. *Annual Review of Immunology*, 11, 571–611. https://doi.org/10.1146/annurev.iy.11.040193.003035

Fisher, M. C., Garner, T. W. J., & Walker, S. F. (2009). Global emergence of *Batrachochytrium dendrobatidis* and amphibian chytridiomycosis in space, time, and host. *Annual Review of Microbiology*, 63, 291–310. https://doi.org/10.1146/annurev.micro.091208.073435

Fites, J. S., Ramsey, J. P., Holden, W. M., Collier, S. P., Sutherland, D. M., Reinert, L. K., Rollins-Smith, L. A. (2013). The invasive chytrid fungus of amphibians paralyzes lymphocyte responses. *Science*, 342, 366–369. https://doi.org/10.1126/science.1243316

Gantress, J., Maniero, G. D., Cohen, N., & Robert, J. (2003). Development and characterization of a model system to study amphibian immune responses to iridoviruses. *Virology*, 311, 254–262. https://doi.org/10.1016/S0042-6822(03)00151-X

Garland, S., Baker, A., Phillott, A. D., & Skerratt, L. F. (2009). BSA reduces inhibition in a TaqMan (R) assay for the detection of *Batrachochytrium dendrobatidis*. *Diseases of Aquatic Organisms*, 92, 113–116. https://doi.org/10.3354/dao02053

Gavrilets, S., Li, H., & Vose, M. D. (2000). Patterns of parapatric speciation. *Evolution*, 54, 1126–1134. https://doi.org/10.1111/j.0014-3820.2000.tb00548.x

Grogan, L. F. (2014). *Understanding Host and Environmental Factors in the Immunology and Epidemiology of Chytridiomycosis in Anuran Populations in Australia*. Douglas, QLD: James Cook University.

Grogan, L. F., Berger, L., Rose, K., Grillo, V., Cashins, S. D., & Skerratt, L. F. (2014). Surveillance for emerging biodiversity diseases of wildlife. *Plos Pathogens*, 10, e1004015. https://doi.org/10.1371/journal.ppat.1004015

Grogan, L. F., Mulvenna, J., Gummer, J. P. A., Scheele, B. C., Berger, L., Cashins, S. D., . . . Trengove, R. D. (2018). Survival, gene and metabolite responses of *Litoria verreauxii alpina* frogs to fungal disease chytridiomycosis. *Scientific Data*. https://doi.org/10.1038/sdata.2018.33

Haas, B. J., Papanicolaou, A., Yassour, M., Grabherr, M., Blood, P. D., Bowden, J., & MacManes, M. D. (2013). *De novo* transcript sequence reconstruction from RNA-seq using the Trinity platform for reference generation and analysis. *Nature Protocols*, 8, 1494–1512. https://doi.org/10.1038/nprot.2013.084

Hansen, K. D., Brenner, S. E., & Dudoit, S. (2010). Biases in Illumina transcriptome sequencing caused by random hexamer priming. *Nucleic Acids Research*, 38, 7.

Harrington, D. P., & Fleming, T. R. (1982). A class of rank test procedures for censored survival-data. *Biometrika*, 69, 553–566. https://doi.org/10.1093/biomet/69.3.553

Harrison, P. W., Mank, J. E., & Wedell, N. (2012). Incomplete sex chromosome dosage compensation in the indian meal moth, plodia interpunctella, based on de novo transcriptome assembly. *Genome Biology and Evolution*, 4, 1118–1126. https://doi.org/10.1093/gbe/evs086

Holden, W. M., & Rollins-Smith, L. A. (2014). Skin bacteria protect newly metamorphosed *Rana sphenocephala* from the emerging fungal pathogen *Batrachochytrium dendrobatidis*. *Integrative and Comparative Biology*, 54, E92–E92.

Huang, Y., Zaas, A. K., Rao, A., Dobigeon, N., Woolf, P. J., Veldman, T., & Carin, L. (2011). Temporal dynamics of host molecular responses differentiate symptomatic and asymptomatic *Influenza A* infection. *Plos Genetics*, 7, e1002234. https://doi.org/10.1371/journal.pgen.1002234

Hunter, D., Pietsch, R., Clemann, N., Scroggie, M., Hollis, G., & Marantelli, G. (2009). Prevalence of the amphibian chytrid fungus (*Batrachochytrium dendrobatidis*) in the Australian Alps. In: Report to the Australian Alps Liaison Committee: January 2009.

Hyatt, A. H. D., Olsen, V., Boyle, D. B., Berger, L., Obendorf, D., Dalton, A., Campbell, R. (2007). Diagnostic assays and sampling protocols for the detection of *Batrachochytrium dendrobatidis*. *Diseases of Aquatic Organisms*, 73, 175–192. https://doi.org/10.3354/dao073175

Jones, P., Binns, D., Chang, H. Y., Fraser, M., Li, W., McAnulla, C., & Pesseat, S. (2014). InterProScan 5: Genome-scale protein function classification. *Bioinformatics*, 30, 1236–1240. https://doi.org/10.1093/bioinformatics/btu031

Kim, B. H., Shenoy, A. R., Kumar, P., Bradfield, C. J., & MacMicking, J. D. (2012). IFN-inducible GTPases in host cell defense. *Cell Host & Microbe*, 12, 432–444. https://doi.org/10.1016/j.chom.2012.09.007

Kinney, V. C., Heemeyer, J. L., Pessier, A. P., & Lannoo, M. J. (2011). Seasonal pattern of *Batrachochytrium dendrobatidis* infection and mortality in *Lithobates areolatus*: affirmation of Vredenburg's "10,000 zoospore rule". *PLoS One*, 6, 10.

Koprivnikar, J., Gibson, C. H., & Redfern, J. C. (2011). Infectious personalities: Behavioural syndromes and disease risk in larval amphibians. *Proceedings of the Royal Society B-Biological Sciences*, 279, 1544–1550.

Langmead, B., Trapnell, C., Pop, M., & Salzberg, S. L. (2009). Ultrafast and memory-efficient alignment of short DNA sequences to the human genome. *Genome Biology*, 10, 10.

Leeds, T. D., Silverstein, J. T., Weber, G. M., Vallejo, R. L., Palti, Y., Rexroad, C. E., Wiens, G. D. (2010). Response to selection for bacterial cold water disease resistance in rainbow trout. *Journal of Animal Science*, 88, 1936–1946. https://doi.org/10.2527/jas.2009-2538

Li, B., & Dewey, C. N. (2011). RSEM: Accurate transcript quantification from RNA-Seq data with or without a reference genome. *BMC Bioinformatics*, 12, 16.

McMahon, T. A., Sears, B. F., Venesky, M. D., Bessler, S. M., Brown, J. M., Deutsch, K., & Civitello, D. J. (2014). Amphibians acquire resistance to live and dead fungus overcoming fungal immunosuppression. *Nature*, 511, 224–227. https://doi.org/10.1038/nature13491

Meyer, D., & Thomson, G. (2001). How selection shapes variation of the human major histocompatibility complex: A review. *Annals of Human Genetics*, 65, 1–26. https://doi.org/10.1046/j.1469-1809.2001.6510001.x

Micallef, L., & Rodgers, P. (2014). EULERAPE: Drawing area-proportional 3-Venn diagrams using ellipses. *PLoS One*, 9, 18.

Moghadam, H. K., Harrison, P. W., Zachar, G., Székely, T., & Mank, J. E. (2013). The plover neurotranscriptome assembly: transcriptomic analysis in an ecological model species without a reference genome. *Molecular Ecology Resources*, 13, 696–705. https://doi.org/10.1111/1755-0998.12096

Murphy, K. P. (2012). *Janeway's Immunobiology* (8th ed). New York, NY: Garland Science.

Murray, K. A., Retallick, R. W., Puschendorf, R., Skerratt, L. F., Rosauer, D., McCallum, H. I., & VanDerWal, J. (2011). Assessing spatial patterns of disease risk to biodiversity: Implications for the management of the amphibian pathogen, *Batrachochytrium dendrobatidis*. *Journal of Applied Ecology*, 48, 163–173. https://doi.org/10.1111/j.1365-2664.2010.01890.x

Murray, K. A., & Skerratt, L. F. (2012). Predicting wild hosts for amphibian chytridiomycosis: Integrating host life-history traits with pathogen environmental requirements. *Human and Ecological Risk Assessment*, 18, 200–224. https://doi.org/10.1080/10807039.2012.632310

Murray, K. A., Skerratt, L. F., Speare, R., & McCallum, H. (2009). Impact and dynamics of disease in species threatened by the amphibian chytrid fungus, *Batrachochytrium dendrobatidis*. *Conservation Biology*, 23, 1242–1252. https://doi.org/10.1111/j.1523-1739.2009.01211.x

Olson, D. H., Aanensen, D. M., Ronnenberg, K. L., Powell, C. I., Walker, S. F., Bielby, J., Fisher, M. C. (2013). Mapping the global emergence of *Batrachochytrium dendrobatidis*, the amphibian chytrid fungus. *PLoS One*, 8, 13.

Osborne, W., Hunter, D., & Hollis, G. (1999). Population declines and range contraction in Australian alpine frogs. In A. Campbell (Ed.), *Declines and disappearances of Australian frogs* (pp. 145–157). Canberra, ACT: Environment Australia.

Pask, J. D., Cary, T. L., & Rollins-Smith, L. A. (2013). Skin peptides protect juvenile leopard frogs (*Rana pipiens*) against chytridiomycosis. *Journal of Experimental Biology*, 216, 2908–2916. https://doi.org/10.1242/jeb.084145

Phillott, A. D., Grogan, L. F., Cashins, S. D., McDonald, K. R., Berger, L. E. E., & Skerratt, L. F. (2013). Chytridiomycosis and seasonal mortality of tropical stream-associated frogs 15 years after introduction of *Batrachochytrium dendrobatidis*. *Conservation Biology*, 27, 1058–1068. https://doi.org/10.1111/cobi.12073

Price, S. J., Garner, T. W., Balloux, F., Ruis, C., Paszkiewicz, K. H., Moore, K., & Griffiths, A. G. (2015). A *de novo* assembly of the common frog (*Rana temporaria*) transcriptome and comparison of transcription following exposure to *Ranavirus* and *Batrachochytrium dendrobatidis*. *PLoS One*, 10, 23.

Ragimekula, N., Varadarajula, N. N., Mallapuram, S. P., Gangimeni, G., Reddy, R. K., & Kondreddy, H. R. (2013). Marker assisted selection in disease resistance breeding. *Journal of Plant Breeding and Genetics*, 1, 90–109.

Ramsey, J. P., Reinert, L. K., Harper, L. K., Woodhams, D. C., & Rollins-Smith, L. A. (2010). Immune defenses against *Batrachochytrium dendrobatidis*, a fungus linked to global amphibian declines, in the South African Clawed Frog, *Xenopus laevis*. *Infection and Immunity*, 78, 3981–3992. https://doi.org/10.1128/IAI.00402-10

Ribas, L., Li, M. S., Doddington, B. J., Robert, J., Seidel, J. A., Kroll, J. S., Fisher, M. C. (2009). Expression profiling the temperature-dependent amphibian response to infection by *Batrachochytrium dendrobatidis*. *PLoS One*, 4, e8408. https://doi.org/10.1371/journal.pone.0008408

Robert, J., Morales, H., Buck, W., Cohen, N., Marr, S., & Gantress, J. (2005). Adaptive immunity and histopathology in frog virus 3-infected *Xenopus*. *Virology*, 332, 667–675. https://doi.org/10.1016/j.virol.2004.12.012

Robert, J., & Ohta, Y. (2009). Comparative and developmental study of the immune system in *Xenopus*. *Developmental Dynamics*, 238, 1249–1270. https://doi.org/10.1002/dvdy.21891

Robinson, M. D., McCarthy, D. J., & Smyth, G. K. (2010). EDGER: A Bioconductor package for differential expression analysis of digital gene expression data. *Bioinformatics*, 26, 139–140. https://doi.org/10.1093/bioinformatics/btp616

Rollins-Smith, L. A., Ramsey, J. P., Reinert, L. K., Woodhams, D. C., Livo, L. J., & Carey, C. (2009). Immune defenses of *Xenopus laevis* against *Batrachochytrium dendrobatidis*. *Frontiers in Bioscience*, S1, 68–91. https://doi.org/10.2741/s8

Rosenblum, E. B., Poorten, T. J., Settles, M., & Murdoch, G. K. (2012). Only skin deep: Shared genetic response to the deadly chytrid fungus in susceptible frog species. *Molecular Ecology*, 21, 3110–3120. https://doi.org/10.1111/j.1365-294X.2012.05481.x

Rosenblum, E. B., Poorten, T. J., Settles, M., Murdoch, G. K., Robert, J., Maddox, N., & Eisen, M. B. (2009). Genome-wide transcriptional response of *Silurana (Xenopus) tropicalis* to infection with the deadly chytrid fungus. *PLoS One*, 4, e6494. https://doi.org/6410.1371/journal.pone.0006494

Rowley, J. J. L., & Alford, R. A. (2007). Behaviour of Australian rainforest stream frogs may affect the transmission of chytridiomycosis. *Diseases of Aquatic Organisms*, 77, 1–9. https://doi.org/10.3354/dao01830

Savage, A. E., & Zamudio, K. R. (2011). MHC genotypes associate with resistance to a frog-killing fungus. *Proceedings of the National Academy of Sciences of the United States of America*, 108, 16705–16710. https://doi.org/10.1073/pnas.1106893108

Scheele, B. C., Guarino, F., Osborne, W., Hunter, D. A., Skerratt, L. F., & Driscoll, D. A. (2014). Decline and re-expansion of an amphibian with high prevalence of chytrid fungus. *Biological Conservation*, 170, 86–91. https://doi.org/10.1016/j.biocon.2013.12.034

Scheele, B. C., Hunter, D. A., Banks, S. C., Pierson, J. C., Skerratt, L. F., Webb, R., & Driscoll, D. A. (2016). High adult mortality in disease-challenged frog populations increases vulnerability to drought. *Journal of Animal Ecology*, 85, 1453–1460. https://doi.org/10.1111/1365-2656.12569

Scheele, B. C., Hunter, D. A., Grogan, L. F., Berger, L. E. E., Kolby, J. E., McFadden, M. S., Driscoll, D. A. (2014). Interventions for reducing extinction risk in chytridiomycosis-threatened amphibians. *Conservation Biology*, 28, 1195–1205. https://doi.org/10.1111/cobi.12322

Scheele, B. C., Hunter, D. A., Skerratt, L. F., Brannelly, L. A., & Driscoll, D. A. (2015). Low impact of chytridiomycosis on frog recruitment enables persistence in refuges despite high adult mortality. *Biological Conservation*, 182, 36–43. https://doi.org/10.1016/j.biocon.2014.11.032

Scheele, B. C., Skerratt, L. F., Grogan, L. F., Hunter, D. A., Clemann, N., McFadden, M., Brannelly, L. (2017). After the epidemic: Ongoing declines, stabilizations and recoveries in amphibians afflicted by chytridiomycosis. *Biological Conservation*, *206*, 37–46. https://doi.org/10.1016/j.biocon.2016.12.010

Searle, C. L., Gervasi, S. S., Hua, J., Hammond, J. I., Relyea, R. A., Olson, D. H., & Blaustein, A. R. (2011). Differential host susceptibility to *Batrachochytrium dendrobatidis*, an emerging amphibian pathogen. *Conservation Biology*, *25*, 965–974. https://doi.org/10.1111/j.1523-1739.2011.01708.x

Skerratt, L. F., Berger, L., Clemann, N., Hunter, D. A., Marantelli, G., Newell, D. A., Brannelly, L. A. (2016). Priorities for management of chytridiomycosis in Australia: Saving frogs from extinction. *Wildlife Research*, *43*, 105–120. https://doi.org/10.1071/WR15071

Skerratt, L. F., Berger, L., Speare, R., Cashins, S., McDonald, K. R., Phillott, A. D., Kenyon, N. (2007). Spread of chytridiomycosis has caused the rapid global decline and extinction of frogs. *EcoHealth*, *4*, 125–134. https://doi.org/10.1007/s10393-007-0093-5

Venesky, M. D., Mendelson, J. R., Sears, B. F., Stiling, P., & Rohr, J. R. (2012). Selecting for tolerance against pathogens and herbivores to enhance success of reintroduction and translocation. *Conservation Biology*, *26*, 586–592. https://doi.org/10.1111/j.1523-1739.2012.01854.x

Voyles, J., Vredenburg, V. T., Tunstall, T. S., Parker, J. M., Briggs, C. J., & Rosenblum, E. B. (2012). Pathophysiology in mountain yellow-legged frogs (*Rana muscosa*) during a chytridiomycosis outbreak. *PLoS One*, *7*, e35374. https://doi.org/10.1371/journal.pone.0035374

Voyles, J., Young, S., Berger, L., Campbell, C., Voyles, W. F., Dinudom, A., Speare, R. (2009). Pathogenesis of chytridiomycosis, a cause of catastrophic amphibian declines. *Science*, *326*, 582–585. https://doi.org/10.1126/science.1176765

Young, S., Whitehorn, P., Berger, L., Skerratt, L. F., Speare, R., Garland, S., & Webb, R. (2014). Defects in host immune function in tree frogs with chronic chytridiomycosis. *PLoS One*, *9*, 16.

Zhao, X. B., & Sandelin, A. (2012). GMD: Measuring the distance between histograms with applications on high-throughput sequencing reads. *Bioinformatics*, *28*, 1164–1165. https://doi.org/10.1093/bioinformatics/bts087

SUPPORTING INFORMATION

Additional Supporting Information may be found online in the supporting information tab for this article.

How to cite this article: Grogan LF, Cashins SD, Skerratt LF, et al. Evolution of resistance to chytridiomycosis is associated with a robust early immune response. *Mol Ecol.* 2018;27:919–934. https://doi.org/10.1111/mec.14493